Electronic Structures of Crystalline and Aqueous Solutions of LiBr, NaBr, KBr, and KBrO₃: In Situ Br L-Edge Near-edge X-ray Absorption Fine Structure

Shuji Matsuo,[†,‡,§] **Ponnusamy Nachimuthu,**[†,‡] **Dennis W. Lindle,**[‡] **Hisanobu Wakita,**[§] **and Rupert C. C. Perera*,**[†,‡]

Center for X-ray Optics, Lawrence Berkeley National Laboratory, Berkeley, California 94720,
Department of Chemistry, University of Nevada, Las Vegas, Nevada 89154, and
Advanced Materials Institute and Department of Chemistry, Faculty of Science,
Fukuoka University, Nanakuma, Jonan-ku, Fukuoka 814-0180, Japan

Received: April 11, 2003; In Final Form: June 28, 2003

The electronic structures of crystalline and aqueous solutions of LiBr, NaBr, KBr, and KBrO₃ were studied using in-situ Br L-edge near-edge X-ray absorption fine structure (NEXAFS) under ambient conditions. The direct observation of the ligand-field potential ($10Dq$) allows the determination of their dependence on the interatomic distances between Br and the first near neighbor in crystalline LiBr, NaBr, KBr, and KBrO₃ and the effect of hydration in the corresponding aqueous solutions. DV–Xα molecular-orbital calculations show that for both crystalline and aqueous solutions of KBr, the transitions occur from Br 2p to the unoccupied states containing mainly 4d orbitals of Br. The 5s and 5p orbitals of Br and 3d orbitals of K also contribute to the unoccupied states in addition to the 4d orbitals of neighbor Br due to the orbital mixing in crystalline KBr.

Various bromine compounds have been widely used in industrial applications such as water purification, agriculture, cars, healthcare, photography, and most importantly, flame-retardants. Investigations have shown that they persist in the environment.[1–4] Many of these bromine compounds are carcinogenic and toxic.[2] Recent in situ X-ray absorption spectroscopic studies show that the inorganic chlorine compounds rapidly transform to less volatile organic compounds with chlorinated phenolic and aliphatic groups as the principal Cl forms during the humidification of plant material. Thus, these processes play a critical role in the cycling of Cl and of several major and trace elements in the environment and may influence human health.[1] Bromine compounds may also undergo similar transformations and subsequently change to harmful substances. Thus, understanding the local electronic structures and the chemical states of the basic bromine compounds in aqueous solution in comparison with corresponding crystalline compounds is extremely important in environmental science and solution chemistry.

The availability of synchrotron-radiation sources for X-ray-absorption spectroscopy has made near-edge X-ray-absorption fine structure (NEXAFS) a powerful tool for detailed understanding of electronic and structural properties of materials lacking long-range order, such as catalysts, inorganic materials, minerals, glasses, organometallic complexes, and biological samples such as enzymes.[5–8] Some of these materials also require in situ NEXAFS measurements. Therefore, we have developed a liquid-phase absorption cell to measure X-ray absorption spectra under ambient conditions. The utility of the absorption cell has been demonstrated previously by studying the optically switchable amorphous metal thin films (Mg–TM,

where TM = Ti, Mn, Co, and Ni) under reaction conditions by the exposure of hydrogen, and Na, Mg, and Al compounds in crystalline state and in aqueous solutions.[9,10]

Previous studies of bromide ions in aqueous solution have been performed only for the Br K absorption region, and it involves multielectron excitations that complicate the analyses of extended X-ray absorption fine structures (EXAFS).[11] Further, it is known for 3d metal compounds that the L-edge absorption spectra are dominated by the strong 2p → 3d dipole transitions and the spectra give fine details.[12] In contrast, the 3d states appear as small prepeaks and the main edge relates to the 4p band in the K-edge absorption spectra.[12] Furthermore, the possibility of measuring structures with a better energy resolution makes L-edge absorption spectra a powerful tool to study materials in more detail.[12] Besides, Br is situated in cubic symmetry in many bromine compounds. Hence the unoccupied 4d orbitals of Br no longer degenerate but split into t₂g and eg states by the ligand-field potential. Photoabsorption studies involving excitations into t₂g and eg states have been widely used to determine the ligand-field potential. These ligand-field potentials provide information on interatomic distances, charge distribution, vibrational amplitudes, and the nature of the material.[13] Thus, we present the first in situ Br L-edge NEXAFS of crystalline and aqueous solution of LiBr, NaBr, KBr, and KBrO₃ using total-fluorescence-yield detection. The discrete variational–Xα (DV–Xα) molecular-orbital calculations were carried out for the Br L₃-edge NEXAFS of crystalline KBr and a 0.1 M aqueous solution to understand the unoccupied electronic structures of Br.[14]
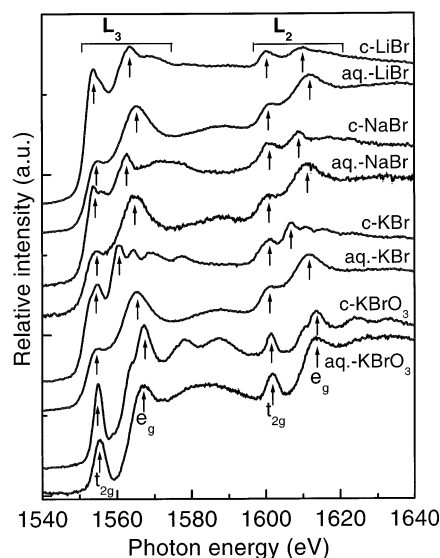
Crystalline compounds (LiBr, NaBr, KBr, and KBrO₃) were purchased from Aldrich Chemical Co. (Milwaukee, WI) and used for the measurements. The 0.1 M aqueous solutions were freshly made with deionized water. The NEXAFS measurements were conducted at Beamline 6.3.1 at the Advanced Light Source (ALS), Lawrence Berkeley National Laboratory.[15] The total-

* Corresponding author. E-mail: RCPerera@lbl.gov.
† Lawrence Berkeley National Laboratory.
‡ University of Nevada.
§ Fukuoka University.

Letters

J. Phys. Chem. B, Vol. 107, No. 46, 2003 **12563**

Figure 1. Bromine L-edge NEXAFS for crystalline and 0.1 M aqueous solutions of LiBr, NaBr, KBr, and $KBrO_3$.

fluorescence-yield was detected using a Hamamatsu GaAsP photodiode (G1127-02). The aqueous solutions were placed in a 6 mm diameter tube containing a 1.5−2.0 mm wide slit. The surface of the solution at the slit in the tube was exposed to the X-ray beam, and fluorescent photons were collected from the solution by the detector (90° to the X-ray beam). For crystalline compounds, a very thin layer of the sample was prepared on a conducting carbon tape and the measurements were performed at grazing incidence to minimize the self-absorption effects in the absorption spectra. Details of the experimental setup are given elsewhere.[9,10] The photon energy was calibrated using the first inflection point of the Al K-edge X-ray absorption spectrum of Al metal and the spectra were normalized to the absorption-edge jumps.[5]

Bromine L-edge X-ray-absorption spectra for crystalline and 0.1 M aqueous solutions of LiBr, NaBr, KBr, and $KBrO_3$ measured at ambient conditions using total-fluorescence-yield detection are shown in Figure 1. These spectra show two relatively broad bands for each 2p spin−orbit-split component, $2p_{3/2}$ (L_3) and $2p_{1/2}$ (L_2). Additional satellite features near the edges and in the postedge regions are clearly visible for the crystalline compounds. Line broadening is found for all the solution spectra when compared to the spectra for the corresponding crystalline compounds. The spectra for 0.1 M aqueous solutions of alkali bromides show features similar to one another with broad satellite features at ~32 eV above the $L_{2,3}$-edges. However, the spectra for the crystalline compounds show features different from each other and the corresponding aqueous solutions. Unlike alkali bromides, the spectrum of aqueous $KBrO_3$ shows the major features observed in crystalline $KBrO_3$, although the satellite features at ~23 and ~32 eV above the $L_{2,3}$-edges broadened contrasting to the features at ~9 eV above the edges that disappeared.

The spin−orbit interaction splits the Br 2p state into $2p_{3/2}$ (L_3) and $2p_{1/2}$ (L_2) states that are ~46.4 eV apart. In alkali bromides and bromates, Br is situated in cubic symmetry, and the ligand-field around Br splits the unoccupied 4d orbitals into lower energy t_{2g} and higher energy e_g states. Thus, the two bands observed for each 2p spin−orbit-split component in the Br L-edge NEXAFS spectra are assigned to the excitation of $2p_{3/2}$ (L_3) and $2p_{1/2}$ (L_2) core electrons into the t_{2g} and e_g states of the unoccupied 4d orbitals. The energy separation between t_{2g}

and e_g states is related to the ligand-field potential, $10Dq = \epsilon(e_g) - \epsilon(t_{2g})$.[13] The values of $10Dq$ obtained from Br L-edge X-ray absorption spectra for crystalline KBr, NaBr, LiBr, and $KBrO_3$ are 7.5, 9.0, 9.6, and 12.0 eV, respectively. The $10Dq$ for 0.1 M aqueous solutions of LiBr, NaBr, and KBr correspond to 10.5 eV. In contrast, the $10Dq$ for 0.1 M aqueous solution of $KBrO_3$ does not deviate significantly from the value of crystalline $KBrO_3$. According to ligand-field theory, the value of $10Dq$ should increase with decreasing metal−ligand bond distance. The first-nearest-neighbor bond distances for crystalline KBr, NaBr, LiBr, and $KBrO_3$ are 3.29, 2.99, 2.74, and 1.65 Å, respectively.[16−18] Thus, the trend in the observed $10Dq$ values from the Br L-edge X-ray absorption spectra are in good agreement with the bond distance reported for crystalline KBr, NaBr, LiBr, and $KBrO_3$. The values of $10Dq$ for 0.1 M aqueous solutions of alkali bromides suggest the metal−Br bonds no longer exist. Instead, alkali bromides in aqueous solution dissociate and hydrate easily, and the alkali cations act simply as counterions. Hence, the $10Dq$ values for 0.1 M aqueous solutions of the alkali bromides have an intermediate value between crystalline LiBr and $KBrO_3$. No change in the $10Dq$ value for 0.1 M aqueous solution from the crystalline $KBrO_3$ indicates that the $[BrO_3]^-$ ion does not dissociate in aqueous solution. The line broadening observed in the X-ray absorption spectra for the solutions suggests the photoabsorption process is faster than atomic motion, so the ligand-field potential experienced by the $2p^{-1}4d$ core excitation is different for each instantaneous arrangement of atoms. The measured line shape, therefore, results from averaging over many excitation energies, each being determined by the ligand-field splitting of a particular atomic arrangement. These results are in accordance with the earlier report on temperature-dependent X-ray absorption spectra at the potassium L-edge of potassium halides.[13] Comparison of Br L-edge NEXAFS spectra for crystalline and aqueous alkali bromides suggest that the satellite features near the $L_{2,3}$-edges and in the postedge regions for the crystalline alkali bromides are associated with transitions into empty states derived from 5s and 5p states of Br and the unoccupied states of the corresponding alkali atoms. Further, the satellite features at ~32 eV above the $L_{2,3}$-edges for the aqueous alkali bromides correspond to the transitions into the empty states of the hydrated H_2O of Br^-. In the Br L-edge NEXAFS spectra for the crystalline $KBrO_3$, the satellite features observed at ~9 eV above the edges, which were absent for the aqueous $KBrO_3$, give an indication that these features occur because of the transitions into the states derived from the empty states of K. The features at ~32 eV above the $L_{2,3}$-edges as also observed for the aqueous alkali bromides are associated with the empty states of O directly bonded to Br, resulting in an enhanced intensity unlike hydrated Br^- in aqueous alkali bromides. However, broadening of these features in aqueous $KBrO_3$ indicates the interaction between $[BrO_3]^-$ ions and H_2O. The features at ~23 eV above the $L_{2,3}$-edges observed for crystalline $KBrO_3$ may be associated with transitions into empty states derived from 5s and 5p states of Br and the unoccupied states of K and O. A drop in intensity of these features in aqueous $KBrO_3$ suggests that the dissociation of K^+ and $[BrO_3]^-$ ions in aqueous solution eliminates the contribution from K to the unoccupied electronic states.

To understand the unoccupied electronic structure of Br more precisely, Br L_3-edge NEXAFS for crystalline KBr and a 0.1 M aqueous solution were analyzed using DV−Xα molecular-orbital calculations.[14] These calculations were performed using a half-occupied core-level (Slater's transition state)[19] and an expanded basis set. For crystalline KBr, calculations were
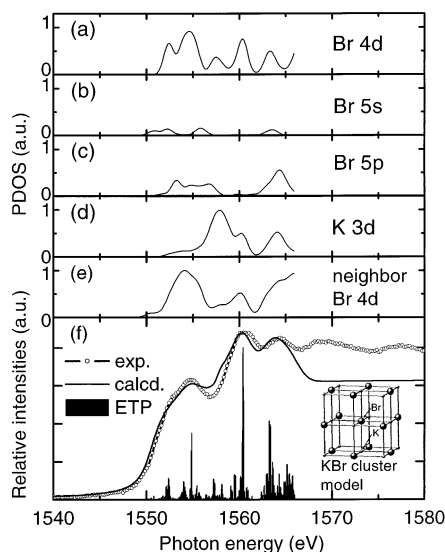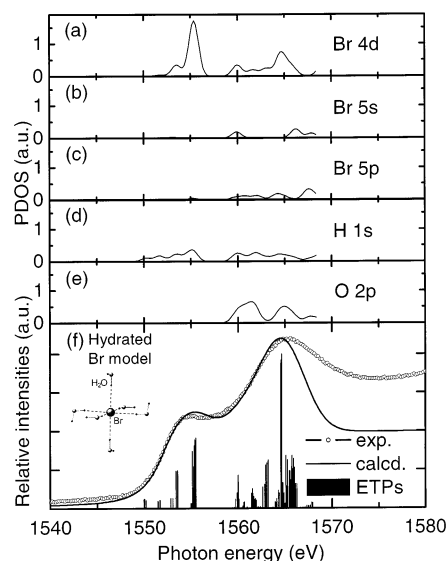
Figure 2. Partial density of states (PDOS) (a)−(e) and the electron transition probabilities (ETP) (f) calculated for the KBr cluster model using the DV−Xα molecular-orbital method. The KBr cluster model is given as the inset. The convoluted ETP using Gaussians (fwhm = 1.25 eV) and an appropriate arctangent function (solid line) is compared with the experimental spectrum (circles).

Figure 3. Partial density of states (PDOS) (a)−(e) and the electron transition probabilities (ETP) (f) calculated for the hydrated Br model using the DV−Xα molecular-orbital method. The hydrated Br model is given as the inset. The convoluted ETP using Gaussians (fwhm = 2.5 eV) and an appropriate arctangent function (solid line) is compared with the experimental spectrum (circles).

performed using a model consisting of 14 potassium and 13 Br atoms with Br atom at the center on the basis of crystallographic data.[16] The KBr exhibits cubic symmetry with a first neighbor distance of 3.29 Å.[16] In the DV−Xα calculations, K and Br atoms were given charges of +1 and −1, respectively. The resulting model was embedded into a Madelung potential field consisting of 702-point charges for the influence of electrostatic energy of the clusters. The atomic orbitals used in the calculations are 1s−5p of K and 1s−5d of Br. The outermost orbitals, 5p of K and 5d of Br, were included in the calculations to suppress the numerical error for the rest of the orbitals, but they were excluded when evaluating the partial density-of-states (PDOS).

For 0.1 M aqueous KBr, the model was made with one Br atom and six water molecules, a model based on earlier work on KBr in solution using X-ray diffraction.[20] This model consists of an octahedral structure with a Br−H bond distance of 2.44 Å and a Br−H−O angle of 175°. In the DV−Xα calculations, Br was given the charge −1. The atomic orbitals used in the calculations (extended basis set) are 1s−5d of Br, 1s−3p of O and 1s−2p of H. The DV−Xα calculations for both models were performed using a numerical integration of 1000 points per atom. Convergence of self-consistent-field iterations was set to 0.001 electrons. Electron transition probabilities (ETP) were evaluated from the dipole matrix element between a core state and unoccupied molecular states.[21] The resultant spectra were convoluted using Gaussians with full-widths-at-half-maximum of 1.25 eV for KBr clusters and 2.5 eV for the hydrated KBr. An absorption continuum described by an arctangent function was used in the simulated spectrum.

The calculated PDOS (a−e), ETP (f, bars), and simulated curve (f, solid line) along with experimental (f, circles) spectra in the energy range 1550−1568 eV using KBr clusters and hydrated Br models are given in Figures 2 and 3 for crystalline and 0.1 M aqueous solution of KBr, respectively. It can be seen that the simulated spectra are in good agreement with the experimental spectra of both crystalline and aqueous KBr. Further, the ETP suggest the transitions occur from Br 2p orbitals to the unoccupied states containing mainly 4d orbitals

of Br for both crystalline and 0.1 M aqueous solution. However, the contribution to the unoccupied states from 5s and 5p orbitals of Br and 3d orbitals of K in addition to the 4d orbitals of neighbor Br for crystalline KBr is larger compared to the contribution from 5s and 5p orbitals of Br, 2p orbitals of O, and 1s of H for 0.1 M aqueous solution. This is due to the long-range ordering of crystalline KBr, which results in mixing of the unoccupied states compared to the aqueous solution. Hence, the satellite features near the edge and in the postedge region are clearly observed for the crystalline KBr due to contributions from 5s and 5p orbitals of Br and 3d orbitals of K in addition to the 4d orbitals of Br to the unoccupied states, unlike the aqueous solution. In contrast, variations in the $10Dq$ values for different alkali bromides and their aqueous solutions are from the degree of interaction between bromide and alkali cations in crystalline compounds and bromide and H_2O in aqueous solutions.

In conclusion, the ligand-field splitting ($10Dq$) of the core excitations of LiBr, NaBr, KBr, and $KBrO_3$, and their corresponding aqueous solutions were studied using in situ Br L-edge NEXAFS under ambient conditions. Ligand-field theory is utilized to understand the dependence of the $10Dq$ values on the interatomic distances between Br and the first near neighbor in crystalline compounds and the hydration in aqueous solutions. DV−Xα molecular-orbital calculations show the transitions occur from Br 2p to the unoccupied states containing mainly 4d orbitals of Br for both crystalline and aqueous solution of KBr. The 5s and 5p orbitals of Br and 3d orbitals of K also contribute to the unoccupied states in addition to the 4d orbitals of neighbor Br due to the orbital mixing in crystalline KBr.

Letters

J. Phys. Chem. B, Vol. 107, No. 46, 2003 **12565**

References and Notes

(1) Myneni, S. C. B. *Science* **2002**, *295*, 1039.

(2) de Boer, J.; Wester, P. G.; Klamer, H. J. C.; Lewis, W. E. Boon, J. P. *Nature* **1998**, *394*, 28 and references therein.

(3) Tittlemier, S. A.; Fisk, A. T.; Hobson, K. A.; Norstrom, R. J. *Environ. Pollut.* **2002**, *116*, 85 and references therein.

(4) Shiao, Y.-H.; Kamata, S. I.; Li, L. M.; Hooth, M. J.; DeAngelo, A. B.; Anderson, L. M.; Wolf, D. C. *Cancer Lett.* **2002**, *187*, 207 and references therein.

(5) *NEXAFS Spectroscopy*; Stöhr, J., Ed.; Springer Series in Surface Science, 25; Springer: New York, 1992.

(6) Chen, J. G. *Surf. Sci. Rep.* **1997**, *30*, 5.

(7) Hashnain, S. S.; Helliwell, J. R.; Kamitsubo, H. *J. Synchrotron Rad.* **1999**, *6*, 121.

(8) Heald, S. M. *X-ray Absorption: Principles, Applications, Techniques of EXAFS, SEXAFS and XANES*; Koningsberger, D. C., Prins, R., Eds.; Wiley: New York, 1988; p 87.

(9) Nachimuthu, P.; Matsuo, S.; Lindle, D. W.; Wakita, H.; Perera, R. C. C. *J. Alloy Compds.*, in press.

(10) Farangis, B.; Nachimuthu, P.; Richardson, T. J.; Slack, J. L.; Perera, R. C. C.; Gullikson, E. M.; Lindle, D. W.; Rubin, M. *Phys. Rev. B* **2003**, *67*, 085106.

(11) Harada, M.; Okada, T.; Watanabe, I. *J. Phys. Chem. B* **2002**, *106*, 34.

(12) de Groot, F. M. F.; Figeiredo, M. O.; Basto, M. J.; Abbate, M.; Petersen, H.; Fuggle, J. C. *Phys. Chem. Miner.* **1992**, *19*, 140.

(13) Sette, F.; Sinkovic, B.; Ma, Y. J.; Chen, C. T. *Phys. Rev. B* **1989**, *39*, 11125.

(14) Adachi, H.; Tsukada, M.; Satoko, C. *J. Phys. Soc. Jpn.* **1978**, *45*, 875.

(15) Underwood, J. H.; Gullikson, E. M. *J. Electron Spectrosc. Relat. Phenom.* **1998**, *92*, 265.

(16) Ott, H. *Z. Kristallogr.* **1926**, *63*, 222.

(17) Templeton, D. H.; Templeton, L. K. *Acta Crystallogr. A* **1985**, *41*, 133.

(18) Ott, H. *Phys. Z.* **1923**, *24*, 209.

(19) Slater, J. C. *Quantum Theory of Molecules and Solids*; McGraw-Hill: New York, 1974.

(20) Ohtaki, H.; Radnai, T. *Chem. Rev.* **1993**, *93*, 1157.

(21) Taniguchi, K.; Henke, B. L. *J. Chem. Phys.* **1976**, *64*, 3021.